XVI International Conference on Computational Plasticity. Fundamentals and Applications
COMPLAS 2021
E. Oñate, D. Peric, M. Chiumenti and Eduardo de Souza Neto (Eds)

A NOVEL GRADIENT-EXTENDED ANISOTROPIC TWO-SURFACE DAMAGE-PLASTICITY MODEL FOR FINITE DEFORMATIONS

HAGEN HOLTHUSEN*, TIM BREPOLS*, STEFANIE REESE* AND JAAN-WILLEM SIMON*

* Institute of Applied Mechanics (IFAM)
RWTH Aachen University
Mies-van-der-Rohe-Str. 1, D-52074 Aachen, Germany
e-mail: holthusen@ifam.rwth-aachen.de, web page: https://www.ifam.rwth-aachen.de

Key words: Anisotropic damage, Damage tensor, Gradient damage-plasticity, Micromorphic approach, Finite strains, Mesh regularization

Abstract. A novel 'two-surface' gradient-extended damage-plasticity model taking into account damage anisotropy in the logarithmic strain space is derived in a thermodynamically consistent manner. In addition, the concept of an additive split is followed, while the weak form of the linear momentum is stated with respect to Lagrangian quantities. Hence, the mapping between these two spaces is additionally addressed here. Moreover, in order to overcome mesh-dependency, the invariants of the second order damage tensor are gradient-enhanced using the micromorphic approach. In addition, some aspects of the numerical implementation are discussed. A numerical example considering an asymmetrically notched specimen illustrates the model's behavior as well as its ability to deliver mesh-independent results.

1 INTRODUCTION

For several decades, much research has been conducted in the field of anisotropic damage from both an experimental and a modeling point of view. Since experimental studies have shown that, for instance, in the case of non-proportional loading paths isotropic damage models reach their limitations, there is an enormous need of anisotropic damage models. Further, if one considers forming processes, besides non-proportional load paths also large deformations occur. Especially in the field of metal forming, coupled models for damage with plasticity at finite deformations are of utmost importance to better understand these processes and to predict local phenomena such as stress peaks.
The field of Continuum Damage Mechanics (CDM) is a well established modeling approach to counteract these problems by means of phenomenological material models. In fact, CDM is still an active field of research and led to coupled anisotropic models at large deformations in the recent past, for instance, for initially isotropic materials using a damage tensor (e.g. [1]) or anisotropic materials using several scalar damage variables (e.g. [2]). Moreover, while for the infinitesimal theory the kinematics in connection with a second order damage tensor are relatively clear, the finite strain theory offers way more

conceptual ways to deal with finite elasto-plasticity combined with anisotropic damage. In addition to the modeling difficulties, it is known that so-called local damage models suffer from severe mesh-dependency when considering structural examples. A possible solution technique is to take additional length scales into account by means of e.g. gradient-extended material model formulations. A certain subclass of those approaches is the micromorphic approach [3, 4], which has proven to avoid mesh-dependency for different cases of damage models (see e.g. [5, 6]).
To this end, a coupled damage-plasticity model using a second order damage tensor in the sense of CDM is discussed. For this purpose, the material formulation takes place in the logarithmic strain space and further assumes the elastic strain to be additively decomposable. Following the micromorphic approach, a novel gradient-extension of the damage tensor's invariants is discussed to counteract mesh-dependency. First, several fundamental aspects for the constitutive framework are presented (Sec. 2), followed by the thermodynamically consistent derivation of the material model in Sec. 3. In Sec. 4, some remarks on the numerical implementation are given, also including a brief description of the transformation of constitutively dependent quantities between logarithmic and Lagrangian space. Finally, a numerical example investigates the proposed gradient-extended material model in Sec. 5.

2 GOVERNING EQUATIONS

Logarithmic strain measures. As widely accepted in the field of finite elasto-plasticity, the total deformation gradient can be multiplicatively decomposed into an elastic and plastic part $\boldsymbol{F} = \boldsymbol{F}_e \boldsymbol{F}_p$. In addition, the polar decomposition of $\boldsymbol{F}_p = \boldsymbol{R}_p \boldsymbol{U}_p$ into a proper orthogonal part and a positive definite stretch part is introduced.
Since the aim of this contribution is to state the material model formulation in terms of logarithmic strain measures, the elastic logarithmic strain is introduced as $\breve{\boldsymbol{\varepsilon}}_e \coloneqq 1/2 \ln(\boldsymbol{F}_e^T \boldsymbol{F}_e)$. However, in order to express the rate of $\breve{\boldsymbol{\varepsilon}}_e$ depending on total and inelastic deformations, the rate of $\boldsymbol{U}_p$ has to be considered rather than its logarithmic counterpart $\ln(\boldsymbol{U}_p)$. To circumvent this problem, the concept of an additive split of the deformation is followed, which is *'surprisingly close'* to the multiplicative version according to [7]. With this approach at hand, the elastic strain is defined as

$$\boldsymbol{\varepsilon}_e \coloneqq \underbrace{\frac{1}{2}\ln(\boldsymbol{C})}_{=:\,\boldsymbol{\varepsilon}} - \underbrace{\frac{1}{2}\ln(\boldsymbol{C}_p)}_{=:\,\boldsymbol{\varepsilon}_p} \tag{1}$$

with the total and plastic right Cauchy-Green tensors $\boldsymbol{C}_{(p)} = \boldsymbol{F}_{(p)}^T \boldsymbol{F}_{(p)}$. Noteworthy, the elastic logarithmic strains $\breve{\boldsymbol{\varepsilon}}_e$ and $\boldsymbol{\varepsilon}_e$ are only equal if and only if $\boldsymbol{C}$ and $\boldsymbol{C}_p$ commute and further $\boldsymbol{F}_p = \boldsymbol{U}_p$ holds. Nevertheless, the split (1) is very well tested for quite different material behaviors in the literature and shows good agreement with experimental observations, even for anisotropic plasticity.

Mapping of second order damage tensor. In the case of a purely elasto-plastic material behavior, the energy ψ is usually assumed as an isotropic function of $\boldsymbol{F}_e^T\boldsymbol{F}_e$ or, in the case of logarithmic strains, as an isotropic function of $\check{\boldsymbol{\varepsilon}}_e$. In contrast, the damage tensor is usually stated with respect to the current or reference configuration and further is assumed to be positive semi-definite. Here, the latter assumption is followed and the referential second order damage tensor $\boldsymbol{D}_r$ is introduced. However, this means that a mapping to the intermediate configuration is required.
Two mapping strategies are considered here, namely symmetry-preserving (e.g. [8]) and mixed-variant mappings (e.g. [9]). While the latter prevent undesired inelastic scaling effects, only the former preserve the symmetry of the damage tensor $\boldsymbol{D}$ in the intermediate configuration in general, which is beneficial for the formulation of ψ in terms of its integrity basis. Each advantage is desirable in the case of damage, which is why a mapping combining both is preferable. Thus, the following mapping is stated

$$\boldsymbol{D} = \boldsymbol{R}_p\boldsymbol{D}_r\boldsymbol{R}_p^T = \boldsymbol{R}_p\boldsymbol{D}_r\boldsymbol{R}_p^{-1} \tag{2}$$

which will be used within this work. For further derivations, please note that the eigenvectors of $\boldsymbol{D}$ and $\boldsymbol{D}_r$ transform according to $\boldsymbol{n}_i^{D} = \boldsymbol{R}_p\,\boldsymbol{n}_i^{D_r}$.

Micromorphic approach. To overcome the severe mesh-dependency, an additional internal length scale is introduced. In this context, the micromorphic approach suggested in [3, 4] offers a quite general way to account for additional gradient influences within the formulation of (local) material models. For this purpose, n additional unknowns - summarized within $\bar{\mathbf{d}} \coloneqq (\bar{d}_1, \dots, \bar{d}_n)$, which is referred to here and in the following as the micromorphic damage vector - are introduced in general. These additional so-called nonlocal variables are strongly coupled to the local variables of the material model, for instance, the damage variable D in the case of scalar isotropic damage models (see e.g. [5]). The gradient influence is then taken into account by an additional field equation - similar to the strong form of linear momentum - introduced for the micromorphic field. In case of damage, this field equation is given as (cf. [5])

$$\mathrm{Div}(\boldsymbol{\Xi}_{0_i}) - \boldsymbol{\xi}_{0_i} = \boldsymbol{0} \quad \text{in } B_0 \tag{3}$$

$$\boldsymbol{\Xi}_{0_i} \cdot \boldsymbol{n}_0 = \boldsymbol{0} \quad \text{on } \partial B_0 \tag{4}$$

with the Lagrangian divergence operator denoted by $\mathrm{Div}(\bullet)$, the 'generalized' stresses $\boldsymbol{\Xi}_{0_i}$ and $\boldsymbol{\xi}_{0_i}$ as well as the outward normal vector $\boldsymbol{n}_0$ with respect to the reference configuration. The domain of the body in the reference configuration is denoted by B_0.

Invariant-based gradient-extension. Several approaches based on the micromorphic one exist in the literature to gradient-enhance local damage material models. While for scalar isotropic damage models it seems natural to gradient-extend the scalar damage variable D, several possibilities exist in the case of anisotropic damage. Besides the approach to extend the components of the damage tensor (e.g. [10]), also the gradient-extension of the damage hardening variable is possible (see [6]). The latter one is beneficial from

a computational point of view, since only one additional degree of freedom has to be considered. However, as discussed in the just mentioned work, this leads to problems for the formulation of the damage yield criterion. To circumvent this situation, the invariants of the second order damage tensor are used for the gradient-extension. Hence, the local damage vector $\mathbf{d} \coloneqq (d_1, d_2, d_3)$ containing the local counterparts to $\bar{d}_i$ is introduced here as

$$d_1 = \mathrm{tr}(\boldsymbol{D}), \quad d_2 = \mathrm{tr}(\boldsymbol{D}^2), \quad d_3 = \mathrm{tr}(\boldsymbol{D}^3). \tag{5}$$

Noteworthy, due to the mapping in Eq. (2), it holds true that $\mathrm{tr}(\boldsymbol{D}^i) = \mathrm{tr}(\boldsymbol{D}_r^i)$ with $i \in \{1, 2, 3\}$. As a consequence, three micromorphic degrees of freedom $\bar{d}_1$, $\bar{d}_2$, $\bar{d}_3$ have to be considered in addition to the displacement field. To the best knowledge of the authors, such an approach based on the invariants of the damage tensor in connection with the micromorphic approach has not yet been used in the literature.

Weak forms. For the numerical implementation, the weak form of both the displacement field and the micromorphic field have to be solved, which read under consideration of Eqs. (3) and (4) in the reference configuration

$$g_u(\boldsymbol{u}, \bar{\mathbf{d}}, \delta\boldsymbol{u}) \coloneqq \int_{B_0} \boldsymbol{S} : \delta\boldsymbol{E} \; \mathrm{d}V - \int_{B_0} \boldsymbol{f}_0 \cdot \delta\boldsymbol{u} \; \mathrm{d}V - \int_{\partial_t B_0} \boldsymbol{t}_0 \cdot \delta\boldsymbol{u} \; \mathrm{d}A = 0 \tag{6}$$

$$g_{\bar{d}}(\boldsymbol{u}, \bar{\mathbf{d}}, \delta\bar{\mathbf{d}}) \coloneqq \int_{B_0} \boldsymbol{\xi}_{0_i} \cdot \delta\bar{\mathbf{d}} \; \mathrm{d}V + \int_{B_0} \boldsymbol{\Xi}_{0_i} : \mathrm{Grad}\left(\delta\bar{\mathbf{d}}\right) \; \mathrm{d}V = 0 \tag{7}$$

with the second Piola-Kirchhoff stress tensor $\boldsymbol{S}$, the short hand notation $\delta\boldsymbol{E} \coloneqq \mathrm{sym}(\boldsymbol{F}^T \mathrm{Grad}(\delta\boldsymbol{u}))$, the volume force $\boldsymbol{f}_0$, the traction $\boldsymbol{t}_0$ and the test functions $\delta\boldsymbol{u}$ and $\delta\bar{\mathbf{d}}$, respectively. Further, the Lagrangian gradient operator is denoted by $\mathrm{Grad}(\bullet)$.

3 CONSTITUTIVE FRAMEWORK

For the constitutive modeling, the plastic logarithmic strain with respect to the intermediate configuration is defined as $\boldsymbol{\eta}_p \coloneqq 1/2 \ln(\boldsymbol{F}_p \boldsymbol{F}_p^T) = \boldsymbol{R}_p \; \boldsymbol{\varepsilon}_p \; \boldsymbol{R}_p^T$. With this quantity at hand, the Helmholtz free energy is assumed to be additively decomposed as

$$\psi = \psi_{\check{e}}(\check{\boldsymbol{\varepsilon}}_e, \boldsymbol{D}) + \psi_p(\boldsymbol{\eta}_p, \kappa_p, \boldsymbol{D}) + \psi_d(\kappa_d) + \psi_h(\boldsymbol{D}) + \psi_{\bar{d}}(\mathbf{d}, \bar{\mathbf{d}}, \mathrm{Grad}(\bar{\mathbf{d}})). \tag{8}$$

Within the assumed form of the energy, $\psi_{\check{e}}$ represents the elastic energy contribution and ψ_p the plastic contribution due to kinematic as well as isotropic hardening with the accumulated plastic strain κ_p. Both are affected by the damage tensor $\boldsymbol{D}$. Furthermore, damage hardening is captured by the damage hardening variable κ_d within the energy ψ_d. The energy associated with ψ_h can be seen as a penalty energy preventing the eigenvalues of $\boldsymbol{D}$ (and thus also $\boldsymbol{D}_r$) from exceeding the value one. Such an approach was already used in the case of anisotropic damage in [6] at small strains. In contrast to the other energies, the integrity basis is not expressed in terms of invariants but rather the eigenvalues of $\boldsymbol{D}$ are used for ψ_h, i.e. $\psi_h = \bar{\psi}_h(D_1, D_2, D_3)$. Nevertheless, this still means that ψ_h is an isotropic function of the second order damage tensor. The last term, namely $\psi_{\bar{d}}$,

accounts for the gradient-extension and further ensures the strong coupling between $\mathbf{d}$ and $\bar{\mathbf{d}}$. This general format can be further specified, having Eq. (5) in mind, since $\mathbf{d}$ is only a function of $\boldsymbol{D}$. Hence, the formulation of this energy contribution can be rewritten as $\psi_{\bar{d}} = \bar{\psi}_{\bar{d}}(\boldsymbol{D}, \bar{\mathbf{d}}, \mathrm{Grad}(\bar{\mathbf{d}}))$.

3.1 Derivation based on the isothermal Clausius-Duhem inequality

For the derivation of thermodynamic driving forces, the micromorphically extended Clausius-Duhem inequality is used

$$-\dot{\psi} + \boldsymbol{T} : \dot{\boldsymbol{\varepsilon}} + \underbrace{\boldsymbol{\xi}_{0_i} \cdot \dot{\bar{\mathbf{d}}} + \boldsymbol{\Xi}_{0_i} : \mathrm{Grad}\left(\dot{\bar{\mathbf{d}}}\right)}_{\text{micromorphic extension}} \geq 0 \tag{9}$$

with the stress power expressed in terms of $\dot{\boldsymbol{\varepsilon}}$ and its stress-like conjugated driving force $\boldsymbol{T}$. Before inserting the total time derivative of ψ into the inequality, one has to note that due to the additive split (1) the elastic strain is defined with respect to the reference configuration. Thus, the elastic energy part in Eq. (8) is no longer a function of $\check{\boldsymbol{\varepsilon}}_e$ but rather $\boldsymbol{\varepsilon}_e$. Since $\boldsymbol{D}$ is located in the intermediate configuration, $\boldsymbol{D}_r$ is utilized in connection with $\boldsymbol{\varepsilon}_e$. Consequently, the elastic energy contribution $\psi_{\check{e}}$ in Eq. (8) is replaced by $\psi_e(\boldsymbol{\varepsilon}_e, \boldsymbol{D}_r)$.
After several mathematical operations, which are omitted here for brevity, the evaluated time derivative of ψ yields the following

$$\begin{aligned} &\left(\boldsymbol{T} - \frac{\partial \psi_e}{\partial \boldsymbol{\varepsilon}_e}\right) : \dot{\boldsymbol{\varepsilon}} + (\boldsymbol{T} - \boldsymbol{X}) : \dot{\boldsymbol{\varepsilon}}_p + \overbrace{(\boldsymbol{Y}_e + \boldsymbol{Y}_p - \boldsymbol{Y}_h - \boldsymbol{Y}_{\bar{d}})}^{=:\boldsymbol{Y}} : \dot{\boldsymbol{D}}_r \\ &+ R_p\, \dot{\kappa}_p + R_d\, \dot{\kappa}_d + \left(\boldsymbol{\xi}_{0_i} - \frac{\partial \psi_{\bar{d}}}{\partial \bar{\mathbf{d}}}\right) \cdot \dot{\bar{\mathbf{d}}} + \left(\boldsymbol{\Xi}_{0_i} - \frac{\partial \psi_{\bar{d}}}{\partial \mathrm{Grad}(\bar{\mathbf{d}})}\right) : \mathrm{Grad}\left(\dot{\bar{\mathbf{d}}}\right) \geq 0. \end{aligned} \tag{10}$$

Following the well-known Coleman-Noll procedure for the stress tensor $\boldsymbol{T}$ as well as similar relations for the 'generalized' stresses in order to fulfill the inequality for arbitrary processes, one may find

$$\boldsymbol{T} = \frac{\partial \psi_e}{\partial \boldsymbol{\varepsilon}_e}, \quad \boldsymbol{\xi}_{0_i} = \frac{\partial \psi_{\bar{d}}}{\partial \bar{\mathbf{d}}}, \quad \boldsymbol{\Xi}_{0_i} = \frac{\partial \psi_{\bar{d}}}{\partial \mathrm{Grad}(\bar{\mathbf{d}})}. \tag{11}$$

Furthermore, the kinematic backstress tensor and the driving force associated with plastic isotropic hardening are defined as

$$\boldsymbol{X} \coloneqq \boldsymbol{R}_p^T \frac{\partial \psi_p}{\partial \boldsymbol{\eta}_p} \boldsymbol{R}_p, \quad R_p \coloneqq -\frac{\partial \psi_p}{\partial \kappa_p}. \tag{12}$$

Analogously, the damage hardening force is introduced as $R_d \coloneqq -\partial \psi_d / \partial \kappa_d$. The remaining driving forces associated with the rate of the second order damage tensor $\boldsymbol{D}_r$ are defined as

$$\boldsymbol{Y}_e \coloneqq -\frac{\partial \psi_e}{\partial \boldsymbol{D}_r}, \quad \boldsymbol{Y}_p \coloneqq -\boldsymbol{R}_p^T \frac{\partial \psi_p}{\partial \boldsymbol{D}} \boldsymbol{R}_p, \quad \boldsymbol{Y}_h \coloneqq \boldsymbol{R}_p^T \frac{\partial \psi_h}{\partial \boldsymbol{D}} \boldsymbol{R}_p, \quad \boldsymbol{Y}_{\bar{d}} \coloneqq \boldsymbol{R}_p^T \frac{\partial \psi_{\bar{d}}}{\partial \boldsymbol{D}} \boldsymbol{R}_p. \tag{13}$$

Noteworthy, the driving forces introduced all have in common that they are defined with respect to the reference configuration. It is further important to note that, since all energies are isotropic functions of their arguments, one can show that the plastic rotation tensor $\boldsymbol{R}_p$ is not needed to compute any of these forces. Moreover, the rate of $\boldsymbol{R}_p$ does not occur within the Clausius-Duhem inequality. Hence, this tensor plays no role in the actual model and remains undetermined, which is considered as an advantage.
To guarantee the non-negativeness of the remaining dissipation inequality, a set of evolution equations for the plastic and damage related quantities are presented in the following. For both processes, associative laws are assumed.

Plastic evolution equations. For simplicity, but without loss of generality, a von Mises-type yield criterion in the so-called effective continuum is assumed which reads

$$\Phi_p = \sqrt{3\tilde{J}_2} - (\sigma_{y0} - \tilde{R}_p) \leq 0 \tag{14}$$

with $J_2 \coloneqq 1/2\ \mathrm{tr}(\mathrm{dev}(\boldsymbol{T} - \boldsymbol{X})^2)$ being the second invariant of the deviator of the driving force and $\tilde{(\bullet)} = (\bullet)|_{\boldsymbol{D}=\boldsymbol{0}}$ refers to effective quantities. The initial yield stress is denoted by σ_{y0}. Based on this criterion, the evolution equations are as follows

$$\dot{\boldsymbol{\varepsilon}}_p = \dot{\gamma}_p \frac{\partial \Phi_p}{\partial \boldsymbol{T}} = \dot{\gamma}_p \frac{3}{\sqrt{12\tilde{J}_2}}\ \mathrm{dev}(\tilde{\boldsymbol{T}} - \tilde{\boldsymbol{X}}) : \mathbb{M}^{-1}, \quad \dot{\kappa}_p = \dot{\gamma}_p \frac{\partial \Phi_p}{\partial R_p} = \frac{\dot{\gamma}_p}{f_d} \tag{15}$$

with the plastic multiplier $\dot{\gamma}_p$. In the above, invertible mappings in terms of a fourth order tensor $\mathbb{M}$ and the scalar degradation function f_d are introduced, which relate effective and damaged quantities, i.e. $\boldsymbol{T} = \mathbb{M} : \tilde{\boldsymbol{T}}$ and $R_p = f_d\ \tilde{R}_p$. Finally, the set of plastic constitutive equations is closed by the Karush-Kuhn-Tucker (KKT) conditions $\Phi_p \leq 0$, $\dot{\gamma}_p \geq 0$ and $\Phi_p \dot{\gamma}_p = 0$.

Damage evolution equations. The damage criterion for the onset of damage is denoted by (cf. [6])

$$\Phi_d = \sqrt{3}\sqrt{\boldsymbol{Y}_+ : \mathbb{A}_d : \boldsymbol{Y}_+} - (Y_0 - R_d) \leq 0. \tag{16}$$

Here, Y_0 denotes the initial damage threshold and further $\boldsymbol{Y}_+ = \sum_{i=1}^{3} \langle Y_i \rangle_M\ \boldsymbol{n}_i^{\boldsymbol{Y}} \otimes \boldsymbol{n}_i^{\boldsymbol{Y}}$ refers to the positive part of the driving force, where Y_i and $\boldsymbol{n}_i^{\boldsymbol{Y}}$ are the eigenvalues and eigenvectors of $\boldsymbol{Y}$, respectively. The Macaulay brackets are given as $\langle(\bullet)\rangle_M = ((\bullet) + |(\bullet)|)/2$. In addition, and in line with [8], the damage yield criterion is extended by a fourth order damage tensor $\mathbb{A}_d$ in order to provide more flexibility for the modeling of damage evolution. Different choices for this tensor are possible, while for the time being the components with respect to the Cartesian basis system are given as $A_{d_{ijkl}} = (\delta_{ik} - D_{r_{ik}})(\delta_{jl} - D_{r_{jl}})$, where δ_{ij} denotes the Kronecker delta. Following again the associative concept, the evolution equations for the damage quantities read as follows

$$\dot{\boldsymbol{D}}_r = \dot{\gamma}_d \frac{\partial \Phi_d}{\partial \boldsymbol{Y}} = \dot{\gamma}_d \frac{3}{Y_0 - R_d} \boldsymbol{Q}_+ (\boldsymbol{I} - \boldsymbol{D}_r) \boldsymbol{Y}_+ (\boldsymbol{I} - \boldsymbol{D}_r) \boldsymbol{Q}_+, \quad \dot{\kappa}_d = \dot{\gamma}_d \frac{\partial \Phi_d}{\partial R} = \dot{\gamma}_d \tag{17}$$

where $\dot{\gamma}_d$ denotes the damage multiplier and $\boldsymbol{Q}_+ = \sum_{i=1}^{3} \langle Y_i \rangle_H \, \boldsymbol{n}_i^{\boldsymbol{Y}} \otimes \boldsymbol{n}_i^{\boldsymbol{Y}}$ with $\langle(\bullet)\rangle_H$ denoting the Heaviside step function. Thus, $\boldsymbol{Y}_+$ can be alternatively expressed as $\boldsymbol{Y}_+ = \boldsymbol{Q}_+ \boldsymbol{Y} \boldsymbol{Q}_+$. In analogy to plasticity, the KKT conditions are introduced as $\Phi_d \leq 0$, $\dot{\gamma}_d \geq 0$ and $\Phi_d \dot{\gamma}_d = 0$. Please note that in Eq. $(17)_1$ it was used that $\sqrt{\boldsymbol{Y}_+ : \mathbb{A}_d : \boldsymbol{Y}_+} = (Y_0 - R_d)/\sqrt{3}$ follows from the KKT conditions for a damage step ($\dot{\gamma}_d > 0$). Although this reformulation does, of course, not change the solution, a division by zero is avoided, which may occur using $\sqrt{\boldsymbol{Y}_+ : \mathbb{A}_d : \boldsymbol{Y}_+}$ within the local Newton iteration.

3.2 Particular choices of Helmholtz free energy terms

While the derivation of the model has been kept quite general so far, in what follows particular choices will be made for the terms in Eq. (8). For the elastic energy, a quadratic form with respect to $\boldsymbol{\varepsilon}_e$ is chosen. Furthermore, as pointed out for instance in [11], the isochoric response of the Helmholtz free energy is assumed to be affected by the anisotropic nature of damage. In contrast, the volumetric part is assumed to be only affected by isotropic damage. Thus, it is influenced by the degradation function f_d already introduced in Eq. $(15)_2$, which is an isotropic function of $\boldsymbol{D}$ (and so of $\boldsymbol{D}_r$). In this regard, a great benefit of logarithmic strains becomes evident, since their decomposition into deviatoric and spherical parts is directly related to the decomposition into distortion and dilatation (see e.g. [12]). Hence, the elastic energy is provided as

$$\psi_e = \mu_e \, \mathrm{tr}\left(\mathrm{dev}(\boldsymbol{\varepsilon}_e)^2 (\boldsymbol{I} - \boldsymbol{D}_r)\right) + f_d \, \frac{K_e}{2} \, \mathrm{tr}\left(\boldsymbol{\varepsilon}_e\right)^2 . \tag{18}$$

In the above, μ_e and K_e denote the shear modulus and bulk modulus, respectively. Similarly, the plastic energy combining kinematic and nonlinear isotropic hardening is denoted by

$$\psi_p = \mu_p \, \mathrm{tr}\left(\mathrm{dev}(\boldsymbol{\eta}_p)^2 (\boldsymbol{I} - \boldsymbol{D})\right) + f_d \, r_p \left(\kappa_p + \frac{\exp(-s_p \, \kappa_p) - 1}{s_p}\right) \tag{19}$$

with μ_p, r_p and s_p being the plastic material parameters. Since a von Mises-type yield criterion is used here, no volumetric response for the backstress needs to be considered. Further, the degradation function is specified as $f_d = 1 - \mathrm{tr}(\boldsymbol{D})/3$. The remaining energies associated with damage are given as

$$\psi_d = r_d \left(\kappa_d + \frac{\exp(-s_d \, \kappa_d) - 1}{s_d}\right) + \frac{1}{2} H_d \, \kappa_d^2, \;\; \psi_h = K_h \sum_{i=1}^{3} \left(-2\sqrt{1 - D_i} - D_i + 2\right) \tag{20}$$

where the material parameters r_d, s_d, H_d and K_h are introduced and both linear and nonlinear isotropic hardening are considered. Finally, the micromorphic contribution to the overall Helmholtz free energy is assumed to be of quadratic type and reads as follows

$$\psi_{\bar{d}} = \frac{1}{2} \sum_{i=1}^{3} \left(H_i \, (d_i - \bar{d}_i)^2\right) + \frac{1}{2} \sum_{i=1}^{3} \left(A_i \, \mathrm{Grad}(\bar{d}_i) \cdot \mathrm{Grad}(\bar{d}_i)\right) \tag{21}$$

with the material parameters H_i and A_i with $i \in \{1,2,3\}$. While for sufficient large H_i the strong couplings between d_i and $\bar{d}_i$ are ensured, A_i introduce additional length scales into the material model accounting for the nonlocal character of damage.

4 REMARKS ON THE NUMERICAL IMPLEMENTATION

The weak forms provided in Eqs. (6) and (7) are solved using the finite element method with standard Q1 elements and are therefore discretized in both space and time. To solve the resulting system of nonlinear equations, the Newton scheme is used on a global level, which requires the material sensitivities $\partial \boldsymbol{S}/\partial \boldsymbol{E}$, $\partial \boldsymbol{S}/\partial \bar{\mathbf{d}}$, $\partial \mathbf{d}/\partial \boldsymbol{E}$, $\partial \mathbf{d}/\partial \bar{\mathbf{d}}$ (more precisely: their algorithmically consistent counterparts are needed), where $\boldsymbol{E}$ denotes the Green-Lagrange strain tensor. Since the material model is derived in the logarithmic strain space, the material sensitivities with respect to the logarithmic strains are obtained first and then transformed to their Lagrangian counterparts. With the relation $\boldsymbol{S} = \boldsymbol{T} : 2\, \partial \boldsymbol{\varepsilon}/\partial \boldsymbol{C}$ at hand, one can find

$$\frac{\partial \boldsymbol{S}}{\partial \boldsymbol{E}} = 4\, \frac{\partial \boldsymbol{\varepsilon}}{\partial \boldsymbol{C}} : \frac{\partial \boldsymbol{T}}{\partial \boldsymbol{\varepsilon}} : \frac{\partial \boldsymbol{\varepsilon}}{\partial \boldsymbol{C}} + \boldsymbol{T} : 4\, \frac{\partial^2 \boldsymbol{\varepsilon}}{\partial \boldsymbol{C} \partial \boldsymbol{C}}, \quad \frac{\partial \boldsymbol{S}}{\partial \bar{\mathbf{d}}} = 2\, \frac{\partial \boldsymbol{\varepsilon}}{\partial \boldsymbol{C}} : \frac{\partial \boldsymbol{T}}{\partial \bar{\mathbf{d}}}, \quad \frac{\partial \mathbf{d}}{\partial \boldsymbol{E}} = 2\, \frac{\partial \mathbf{d}}{\partial \boldsymbol{\varepsilon}} : \frac{\partial \boldsymbol{\varepsilon}}{\partial \boldsymbol{C}} \tag{22}$$

where it was utilized that $\partial \boldsymbol{\varepsilon}/\partial \boldsymbol{C}$ possess both minor and major symmetry. For the derivation of the transformation - at least for the purely mechanical part - the reader is kindly referred to [13]. Noteworthy, the sensitivity $\partial \mathbf{d}/\partial \bar{\mathbf{d}}$ does not need to be transformed.
The local residual functions are obtained by the discretized evolution Eqs. (15) and (17) within a time interval $t \in [t_n, t_{n+1}]$ using the backward Euler method and additionally the yield criteria (14) and (16). Thus, the internal variables which have to be solved are $\Delta t \dot{\gamma}_{p_{n+1}}$, $\boldsymbol{\varepsilon}_{p_{n+1}}$, $\Delta t \dot{\gamma}_{d_{n+1}}$, $\boldsymbol{D}_{r_{n+1}}$. Note that this is sufficient to ensure plastic incompressibility. However, in order to avoid a division by zero for the local Jacobian, the (modified) damage criterion solved on a material point level reads: $\bar{\Phi}_d = 3\, \boldsymbol{Y}_+ : \mathbb{A}_d : \boldsymbol{Y}_+ - (Y_0 - R_d)^2 = 0$. It is worth noting that, if damage is active ($\dot{\gamma}_d > 0$), $\bar{\Phi}_d$ can be obtained by means of an equivalence transformation of Φ_d. For the solution strategy, a combination of the classical trial step procedure in combination with an active-set search strategy is pursued. The local Jacobian as well as the material sensitivities within the logarithmic space are obtained with the help of the implicit function theorem and the algorithmic differentiation tool *AceGen*. Thus, the four tangent operators for the finite element method can be computed automatically in a consistent manner.

5 NUMERICAL EXAMPLE

In order to investigate the model's behavior as well as its ability to deliver mesh-independent results, an asymmetrically notched specimen is studied. The computation is conducted under plane strain conditions using 2D quadrilateral finite elements. The boundary value problem is taken from the literature [14] and is illustrated in Fig. 1. The specimen is clamped at its left side and loaded by a concentrated force at the node in the middle of the right edge. In addition, the horizontal displacement degrees of freedom at this very edge are constrained in such a way that they deform in the same way as the

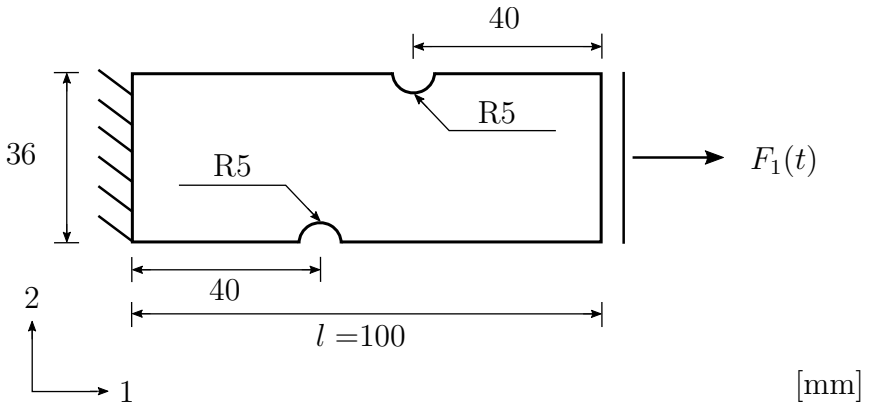

Figure 1: Geometry and boundary value problem.

node loaded by the single load does.
The material parameters for this example are partly taken from [5], otherwise chosen as: $\mu_e = 55000$ [MPa], $K_e = 61666.\bar{6}$ [MPa], $\mu_p = 62.5$ [MPa], $r_p = 125$ [MPa], $s_p = 5$ [-], $\sigma_{y0} = 100$ [MPa], $H_d = 1$ [MPa], $r_d = 5$ [MPa], $s_d = 100$ [-], $K_h = 0.1$ [MPa], $Y_0 = 2.5$ [MPa] as well as $A_i = 75$ [MPa mm^2] and $H_i = 10^5$ [MPa] with $i \in \{1, 2, 3\}$.
A mesh convergence study using 1624, 3592, 9667, 12704 and 13955 finite elements is conducted and shown in Fig. 2, where u_1 corresponds to the displacement of the right edge. A clear trend towards a solution with a finite amount of energy dissipation can be observed. Noteworthy, mesh refinement is strongly performed between the two notches.
In the process, damage starts to evolve at both notches and from that on progresses towards the interior of the specimen. Three stages during this process are shown in Fig. 3 for the damage component $D_{r_{11}}$, where these stages are indicated by black rectangles in Fig. 2. The corresponding accumulated plastic strain is shown as well. The remaining damage components of interest ($D_{r_{22}}$, $D_{r_{33}}$, $D_{r_{12}}$) are not shown here for brevity, however, $D_{r_{22}}$ evolves quite similar to $D_{r_{11}}$, whereas $D_{r_{33}}$ reaches merely a value of approximately 0.9 due to the plane strain conditions. This is also the reason why the load-displacement curve only drops to slightly less than ten percent of the maximum load achieved. Nevertheless, this can be considered as a 'fully broken' state, since a clear crack path can be observed. Furthermore, in Fig. 4 the convergence of the damage contour plots of two exemplary meshes at the end of the simulation is shown. Although there are slight differences in the area of the upper notch visible, these can be considered as negligibly small.

6 CONCLUSION

In this work, a thermodynamically consistent damage-plasticity model accounting for the anisotropic nature of damage by means of a second order damage tensor was presented. Moreover, a novel gradient-enhanced framework based on the invariants of the second order damage tensor and the micromorphic approach was discussed, in order to tackle mesh-sensitivities caused by damage localization. Hence, three degrees of freedom in addition to the displacement field have to be considered within the finite element

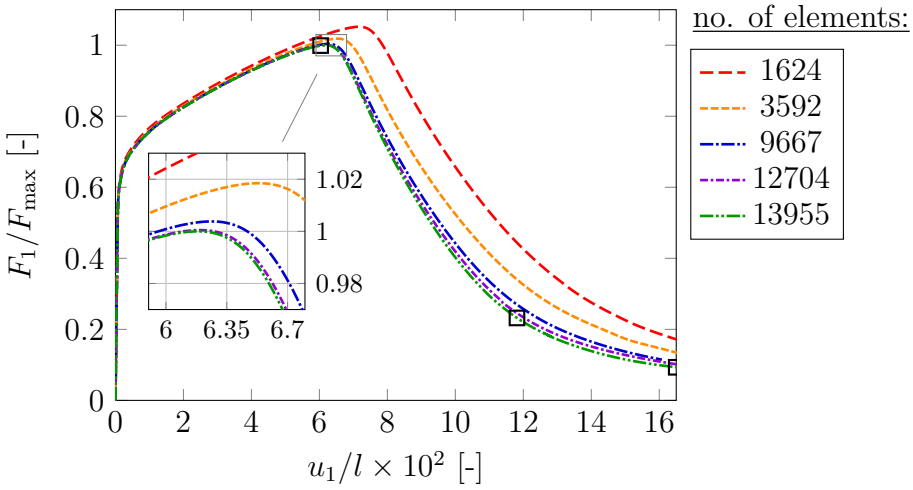

Figure 2: Normalized load-displacement curves ($F_{\max} = 5.4631$ [kN]).

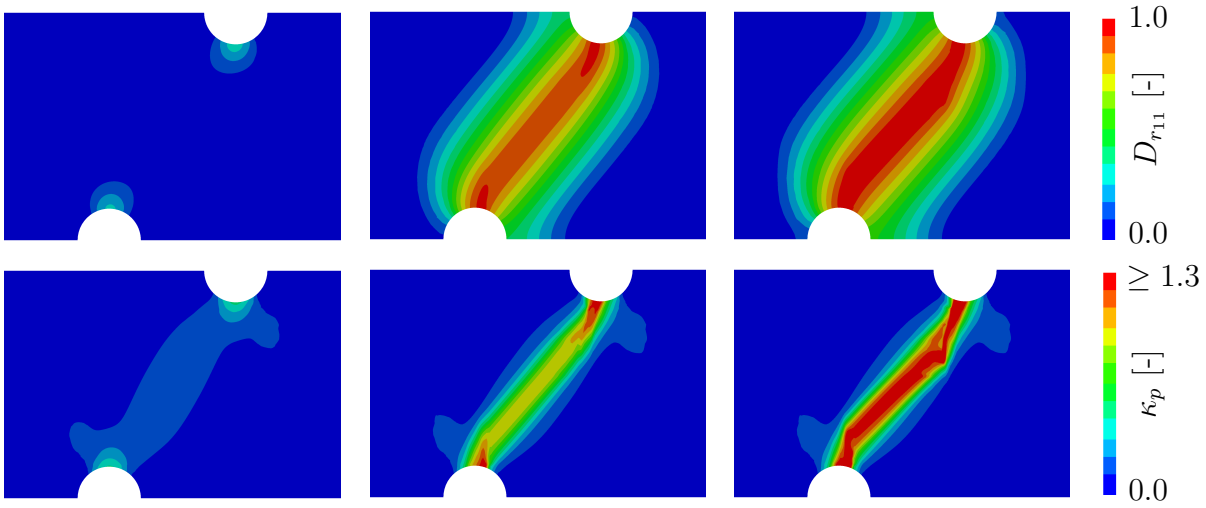

Figure 3: Three different stages of damage component $D_{r_{11}}$ and accumulated plastic strain κ_p for the finest mesh (13955 elements). The stages are indicated by black rectangles within Fig. 2.

method.

Based on the extended Clausius-Duhem inequality, expressions for the conjugated forces associated with the gradient-extension and the stress tensor were derived. Within this modeling approach, both logarithmic strains and an additive split of the elastic strain were utilized for the kinematics. The remaining dissipation inequality is fulfilled for arbitrary processes by means of associative evolution equations for the damage and plastic variables, respectively. In order to be applicable in standard finite element formulations based on Lagrangian quantities, the transformation from the logarithmic strain space was additionally addressed, in particular the transformation of the (algorithmic consistent) tangent operators. Finally, a numerical example demonstrated the behavior of the pro-

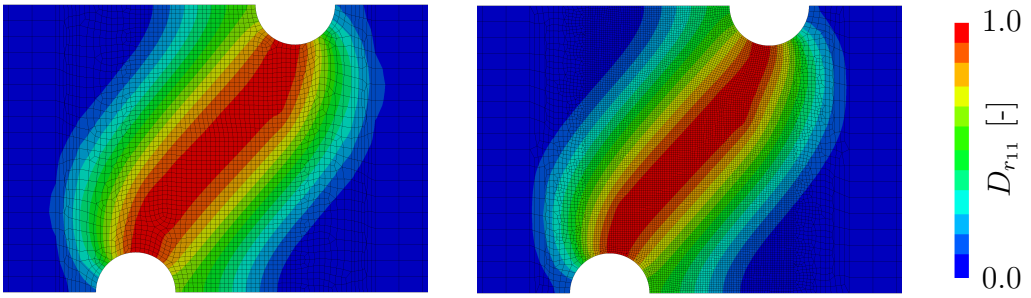

Figure 4: Exemplary comparison of damage contour plots $D_{r_{11}}$ for different mesh refinements at the end of the simulation ($u_1 = 16.5$ [mm]) plotted with the corresponding mesh.

posed model on a structural level as well as the ability to cure the mesh-dependency. It may be mentioned that a much more detailed study is currently in progress. In addition, the consideration of finite element technology could be interesting in order to reduce the computational effort (e.g. [15]).

Acknowledgements
Financial support of the projects RE 1057/46-1 (Project number 404502442) by the German Science Foundation (DFG) is gratefully acknowledged. Additionally, S. Reese and T. Brepols acknowledge the funding of the project RE 1057/51-1 (DFG, Project number 453715964).

REFERENCES

[1] H. Badreddine, K. Saanouni, and T. D. Nguyen. Damage anisotropy and its effect on the plastic anisotropy evolution under finite strains. *International Journal of Solids and Structures*, (2015) **63**:11–31.

[2] H. Holthusen, T. Brepols, S. Reese, and J.-W. Simon. An anisotropic constitutive model for fiber-reinforced materials including gradient-extended damage and plasticity at finite strains. *Theoretical and Applied Fracture Mechanics*, (2020) **108**:102642.

[3] S. Forest. Micromorphic approach for gradient elasticity, viscoplasticity, and damage. *Journal of Engineering Mechanics*, (2009) **135**(3):117–131.

[4] S. Forest. Nonlinear regularization operators as derived from the micromorphic approach to gradient elasticity, viscoplasticity and damage. *Proceedings of the Royal Society A: Mathematical, Physical and Engineering Sciences*, (2016) **472**(2188):20150755.

[5] T. Brepols, S. Wulfinghoff, and S. Reese. A gradient-extended two-surface damage-plasticity model for large deformations. *International Journal of Plasticity*, (2020) **129**:102635.

[6] M. Fassin, R. Eggersmann, S. Wulfinghoff, and S. Reese. Gradient-extended anisotropic brittle damage modeling using a second order damage tensor – theory, implementation and numerical examples. *International Journal of Solids and Structures*, (2019) **167**:93 – 126.

[7] C. Miehe, N. Apel, and M. Lambrecht. Anisotropic additive plasticity in the logarithmic strain space: modular kinematic formulation and implementation based on incremental minimization principles for standard materials. *Computer Methods in Applied Mechanics and Engineering*, (2002) **191**(47):5383 – 5425.

[8] S. Reese, T. Brepols, M. Fassin, L. Poggenpohl and S. Wulfinghoff. Using structural tensors for inelastic material modeling in the finite strain regime – a novel approach to anisotropic damage. *Journal of the Mechanics and Physics of Solids*, (2021) **146**:104174.

[9] S. Murakami. Mechanical Modeling of Material Damage. *Journal of Applied Mechanics*, (1988) **55**(2):280–286.

[10] K. Langenfeld and J. Mosler. A micromorphic approach for gradient-enhanced anisotropic ductile damage. *Computer Methods in Applied Mechanics and Engineering*, (2020) **360**:112717.

[11] R. Desmorat. Anisotropic damage modeling of concrete materials. *International Journal of Damage Mechanics*, (2016) **25**(6):818–852.

[12] J. C. Criscione, J. D. Humphrey, A. S. Douglas and W. C. Hunter. An invariant basis for natural strain which yields orthogonal stress response terms in isotropic hyperelasticity. *Journal of the Mechanics and Physics of Solids*, (2000) **48**(12):2445-2465.

[13] C. Miehe and M. Lambrecht. Algorithms for computation of stresses and elasticity moduli in terms of seth–hill's family of generalized strain tensors. *Communications in Numerical Methods in Engineering*, (2001) **17**(5):337–353.

[14] T. Brepols, S. Wulfinghoff, and S. Reese. Gradient-extended two-surface damage-plasticity: Micromorphic formulation and numerical aspects. *International Journal of Plasticity*, (2017) **97**:64–106.

[15] O. Barfusz, T. van der Velden, T. Brepols, H. Holthusen, and S. Reese. A reduced integration-based solid-shell finite element formulation for gradient-extended damage. *Computer Methods in Applied Mechanics and Engineering*, (2021) **382**:113884.